ELSEVIER

Journal of Alloys and Compounds 446–447 (2007) 39–43

Journal of ALLOYS AND COMPOUNDS

www.elsevier.com/locate/jallcom

# Hydrogen storage properties in a composite of lithium hydride and boron nitride with hydrocarbon groups

Hiroki Miyaoka [a], Takayuki Ichikawa [b,*], Yoshitsugu Kojima [b], Hironobu Fujii [b]

[a] *Department of Quantum Matter, ADSM, Hiroshima University, 1-3-1 Kagamiyama, Higashi-Hiroshima 739-8530, Japan*
[b] *Institute for Advanced Materials Research, Hiroshima University, 1-3-1 Kagamiyama, Higashi-Hiroshima 739-8530, Japan*

Received 24 October 2006; received in revised form 16 March 2007; accepted 16 March 2007
Available online 5 April 2007

**Abstract**

We synthesized $BN^{nano}CH_x$ by ball-milling hBN under methane atmosphere. This $BN^{nano}CH_x$ product itself desorbed not only hydrogen but also hydrocarbons in a wide temperature range from 300 to 900 °C. Moreover, Fourier transform infrared (FT-IR) spectroscopy for $BN^{nano}CH_x$ indicated the existence of the C–H bonding in the material. On the analogy of the $C^{nano}H_x$–LiH composite reported before, we prepared the composite of $BN^{nano}CH_x$ and LiH. This composite successfully desorbed hydrogen around 200 °C, in which the emission of the hydrocarbon gases was strongly suppressed. Thermodynamic and structural properties of the composite showed an interaction between the C–H groups and LiH. Thus we found that the $BN^{nano}CH_x$–LiH composite is a new hydrogen storage material.


*Keywords:* Hydrogen absorbing materials; Nanostructured materials; Solid state reactions; Thermodynamic properties; Thermal analysis

## 1. Introduction

At present, a lot of scientists are researching on high performance hydrogen storage materials to establish suitable transportation technologies for a clean and sustainable society. Recently, hydrogen storage materials composed of light elements have been paid much attention as an on-board application because it is expected that gravimetrically and volumetrically high densities of hydrogen would be realized.

Since Dillon et al. reported on the hydrogen storage properties of single-walled carbon nano-tube in 1997 [1], various carbon based materials have been investigated all over the world. Among them, we have focused on nano-structural hydrogenated graphite ($C^{nano}H_x$) and have investigated the hydrogen storage properties [2–7]. The $C^{nano}H_x$ product was synthesized from graphite powder by mechanical ball-milling method under hydrogen atmosphere for 80 h. The nano-structure and hydrogenation were induced during ball-milling process simultaneously. Therefore, $C^{nano}H_x$ possessed high hydrogen storage capacity of 7 mass% because hydrogen atoms were chemisorbed at the edges of graphene sheet as –CH, $–CH_2$ or $–CH_3$ groups in nano-size grains produced by mechanical ball-milling. In fact, these hydrocarbon groups have been detected by neutron scattering measurements [8] and IR absorption spectroscopy [9]. From thermodynamic points of view, this product desorbed hydrogen as well as some hydrocarbons such as $CH_4$ and $C_2H_6$ in the temperature range from 300 to 900 °C. However, the hydrogen desorption temperatures were recognized to be so high for practical use. Furthermore, it is difficult to rehydrogenate this product under a moderate pressure and temperature condition for using as an on-board application, because a graphitization of the sample proceeded after the dehydrogenation with increase in the temperature above 700 °C [5].

In a recent study, the $C^{nano}H_x$ material was mixed with each alkali (-earth) metal hydride by ball-milling, yielding composite materials (metal–C–H materials) [10–13]. The metal–C–H material composed of $C^{nano}H_x$ and LiH released hydrogen around 350 °C within few hours. Additionally, the hydrocarbon desorption from the $C^{nano}H_x$–LiH composite was strongly suppressed compared with that from the $C^{nano}H_x$ material itself [11]. It was considered that the polarized groups such as –CH, $–CH_2$ or $–CH_3$ at the edges of graphene in the $C^{nano}H_x$ and the ionic crystal of LiH are destabilized by interacting with each other, leading to release of hydrogen gas

* Corresponding author. Tel.: +81 82 424 5744; fax: +81 82 424 5744.
*E-mail address:* tichi@hiroshima-u.ac.jp (T. Ichikawa).

0925-8388/$ – see front matter © 2007 Elsevier B.V. All rights reserved.
doi:10.1016/j.jallcom.2007.03.140

at lower temperature compared with that of each component [14].

It is well known that boron nitride (BN) forms various structures such as layered structure and nano-tube according to different synthesizing methods, considering that BN materials would be similar to carbon materials. So far, hydrogen storage properties of BN nano-tube [15–17] and hexagonal (hBN) [18–20] have been investigated as well as the carbon materials. As reported by Wang *et al*., it was clarified that hBN could absorb about 2 mass% $H_2$ as a stable hydrogenated state and formed nano-structure by mechanical ball-milling under hydrogen atmosphere. Accordingly, hydrogen atoms would be absorbed in the nano-structural hBN ($BN^{nano}$) as a chemisorbed state at the edges of layered structure composed of boron (B)–nitrogen (N) hexatomic ring.

On the basis of above background, we have synthesized a new hydrogen storage material composed of hBN based material and LiH. It is expected that a chemical adsorption of the polarized hydrocarbon groups are induced at the edges of the layered structure in hBN by mechanical ball-milling under methane ($CH_4$) atmosphere, where the hydrocarbonized hBN product is named as $BN^{nano}CH_x$. The nano-composite of $BN^{nano}CH_x$ and LiH synthesized by mixing both components is expected to desorb hydrogen gas at much lower temperature than that of each material by an interaction between the polarized groups and the ionic structure as well as the hydrogen desorption reaction of the metal–C–H materials.

In this paper, $BN^{nano}CH_x$ and the $BN^{nano}CH_x$–LiH composite are characterized from thermodynamic, structural and optical points of view. Based on the results of thermal gas desorption analysis and structural examination of these materials, the hydrogen desorption behavior of this composite is discussed to understand why hydrogen is desorbed at lower temperature than the decomposition temperatures of each component.

## 2. Experimental

$BN^{nano}CH_x$ materials were synthesized by ball-milling hexagonal boron nitride (hBN) powder (99%, Aldrich) using a rocking (vibrating) ball-mill apparatus (SEIWA GIKEN Co. Ltd., RM-10). Then, 300 mg of hBN powder and 20 $ZrO_2$ balls with 8 mm in diameter were put into a milling vessel with an inner volume of ~30 $cm^3$ made of Cr steel (SKD-11) and the hBN powder was milled under 1 MPa methane ($CH_4$) at room temperature, where the milling times were chosen to be 8, 32 and 80 h. As references, $BN^{nano}H_x$ and $C^{nano}H_x$ materials were also prepared by using the rocking mill apparatus from hBN and graphite (99.999%, STREAM CHEMICALS) powder, respectively, where the ball-milling was performed for 80 h under 1 MPa hydrogen ($H_2$) atmosphere. After that, the composite of the $BN^{nano}CH_x$ material and LiH were mechanically milled for 2 h under the 1 MPa $H_2$ atmosphere by using a planetary (rotating) ball-mill apparatus (Fritsch, P7), in which totally 300 mg of 80 h milled $BN^{nano}CH_x$ and LiH mixture and 20 $ZrO_2$ balls put into the Cr steel vessel and the molar ratio of the $BN^{nano}CH_x$ and LiH was chosen to be 1:1.

All the samples were handled in a glovebox (Miwa MFG, MP-P60W) filled with purified argon (>99.9999%) to avoid an oxidation and pollution due to water vapor. Thermal gas desorption properties and thermodynamic properties of as-prepared samples were examined by a thermal desorption mass spectroscopy (TDMS) (Anelva, M-QA200TS) connected to thermogravimetry (TG) and differential thermal analysis (DTA) (Rigaku, TG8120). Especially, this equipment is installed inside the glovebox to minimize an influence of exposing the samples to air. In the thermal analysis, high purity helium gas (>99.9999%) was flowed as a carrier gas, and the heating rate was fixed at 5 °C/min for all the samples studied in this work. Structural properties of all samples were examined by an X-ray diffraction measurement (XRD) (Rigaku, RINT-2100, Cu Kα radiation), where the samples were covered by a polyimide sheet (Kapton®, Du Pont-Toray Co. Ltd.) in the glovebox to avoid an oxidation during the XRD measurements. The FT-IR measurements were performed by using a diffuse reflection cell to examine IR active stretching modes in the $BN^{nano}CH_x$ materials and the $BN^{nano}H_x$ and $C^{nano}H_x$ materials as reference. For IR absorption spectroscopy, the hBN based samples and $C^{nano}H_x$ were diluted by KBr down to 10 and 1 mass%, respectively. Moreover, the FT-IR equipment is also installed inside a home-made glovebox filled with purified argon.

## 3. Results and discussion

### 3.1. Characterization of $BN^{nano}CH_x$

Fig. 1 shows the thermal gas desorption spectra and the TG profiles of the $BN^{nano}CH_x$ products synthesized by ball-milling for 8 h (a), 32 h (b) and 80 h (c). It is considered that mass number 2, 16 and 28 in Fig. 1 consist with hydrogen, methane ($CH_4$) and ethane ($C_2H_6$), respectively, where each fragment of above gases is also observed in the TDMS measurement. All the $BN^{nano}CH_x$ products desorbed hydrogen and hydrocarbons in the temperature range from 300 to 900 °C without $NH_3$ or $BH_3$. The peak temperatures of hydrogen and hydrocarbons desorption are located around 750 and 650 °C, respectively. As shown in the TG profiles, weight loss of $BN^{nano}CH_x$ was increased from 5.0 to 9.5 mass% with increase in the milling time from 8 to 80 h. These results indicate that the number of hydrocarbon groups at

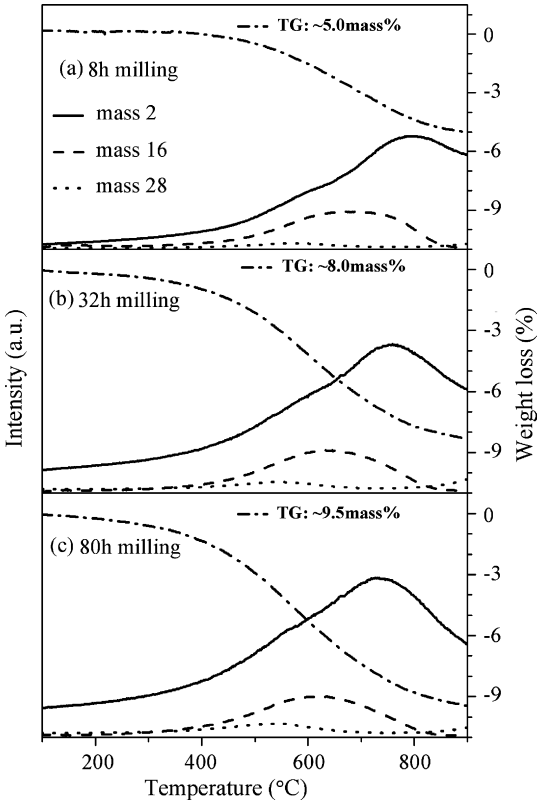


Fig. 1. Thermal gas desorption spectra of hydrogen (mass 2) and hydrocarbons (mass 16 and 28) from the $BN^{nano}CH_x$ materials and TG profiles corresponding to weight loss with increase in a temperature up to 900 °C (dashed and dotted line); (a) 8 h milled, (b) 32 h milled and (c) 80 h milled $BN^{nano}CH_x$.

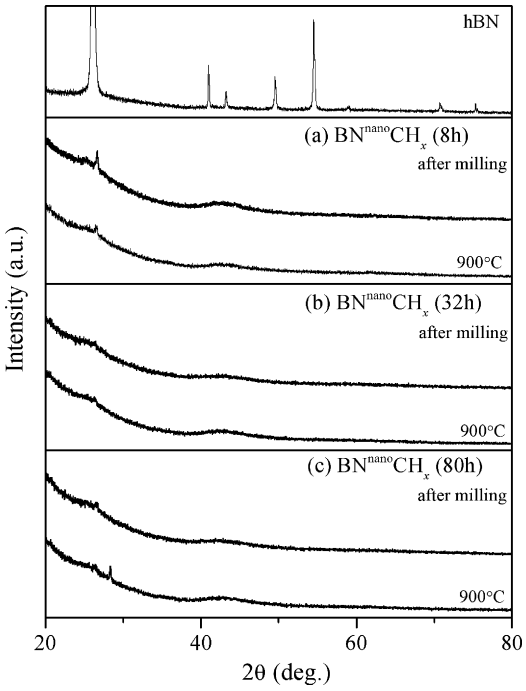


Fig. 2. XRD profiles of the $BN^{nano}CH_x$ materials after milling (upper) and after heating up to 900 °C (lower); (a) 8 h milled, (b) 32 h milled and (c) 80 h milled $BN^{nano}CH_x$.

the edges of the hBN layers is enhanced with increase in the milling time because these edges would be produced during mechanical milling process. In the DTA measurement, no clear peaks corresponding to endothermic or exothermic reaction was found around the peak temperatures of the gas desorption, indicating that the enthalpy of reaction with releasing hydrogen or hydrocarbons in the $BN^{nano}CH_x$ product is quite small.

Figs. 2(a)–(c) shows the XRD patterns of the $BN^{nano}CH_x$ product synthesized by 8, 32 and 80 h milling, and as references, the profile corresponding to hBN is added. As shown in Fig. 2 (a), some small peaks and diffuse peaks corresponding to hBN were found around 26° and 43° in the XRD pattern, respectively. However, it seems that the layered structure of the hBN has almost been destroyed after only 8 h milling. Moreover, in the case of the $BN^{nano}CH_x$ milled for more than 32 h, no peaks were observed in the XRD profiles as shown in Fig. 2(b) and (c). These facts indicate that nano-structures in hBN are induced by ball-milling. In addition, the crystallization of hBN was not significantly occurred by the annealing up to 900 °C for all the $BN^{nano}CH_x$ products as shown in Fig. 2, where it seemed that some extra diffraction peaks around 26° or 28° correspond to quite small amount of impurities such as hBN or boron oxides.

Fig. 3 shows an FT-IR spectrum of the 80 h milled $BN^{nano}CH_x$ material. As references, the results of the $C^{nano}H_x$ and $BN^{nano}H_x$ materials are also shown in Fig. 3. In the spectrum of $BN^{nano}CH_x$, some peaks were found at ~3440, 3000–2840 and ~2500 $cm^{-1}$. The peaks located from 3000 to 2840 $cm^{-1}$ correspond to the C–H stretching modes of the polarized $–CH_2$, $–CH_3$ groups because these peak positions are in the same region as those in the FT-IR spectrum of $C^{nano}H_x$ [9]. Therefore, it is con-

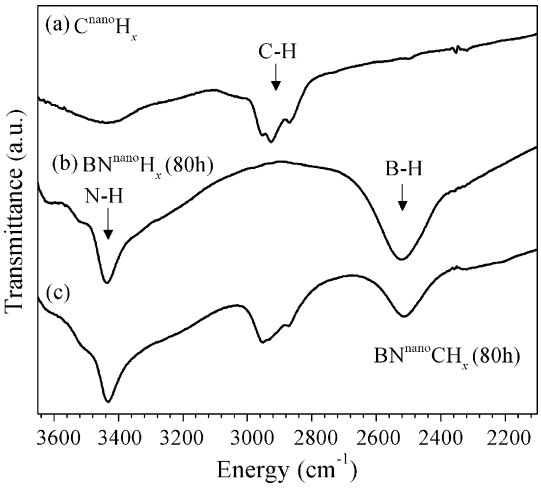


Fig. 3. FT-IR absorption spectra of $BN^{nano}CH_x$ and reference materials; (a) the $C^{nano}H_x$, (b) the $BN^{nano}H_x$ and (c) the $BN^{nano}CH_x$ material, which are synthesized by mechanical milling for 80 h.

firmed that hydrocarbon (CH) groups are located at the edges of hBN layer by using ball-milling method under methane atmosphere. The FT-IR spectrum of the $BN^{nano}H_x$ material revealed two peaks at ~3440 and ~2500 $cm^{-1}$ without any peaks corresponding to C–H stretching mode located 3000~2840 $cm^{-1}$. On the other hand, the peaks corresponding to the N–H and B–H stretching modes were observed at 3150–3500 $cm^{-1}$ [20–22] and around 2500 $cm^{-1}$ [19,23], respectively. In fact, the O–H stretching mode could be appeared as a quite broad peak around 3420 $cm^{-1}$ in Fig. 3(a). However, the peak sharpness between the O–H and the N–H modes is quite different. Therefore, from the comparison between the FT-IR spectra of $BN^{nano}CH_x$ and $BN^{nano}H_x$, the peaks of $BN^{nano}CH_x$ at ~3440 and ~2500 $cm^{-1}$ were assigned to N–H and B–H stretching modes, respectively.

FT-IR results indicate that the $BN^{nano}CH_x$ material possesses three polarized groups corresponding to N–H, C–H and B–H stretching modes. Therefore, it is suggested that hydrogen atoms or hydrocarbon groups dissociated from $CH_4$ during the mechanical milling are chemisorbed as the polarized N–H, C–H and B–H groups at the edges of layers in the nano-structured hBN. On the basis of above results, these polarized groups in $BN^{nano}CH_x$ should be destabilized by mixing with LiH just like hydrogen desorbing reaction of the $C^{nano}H_x$ and LiH composite [10,11].

### 3.2. Hydrogen desorption properties of the Li–BN–C–H composite

Fig. 4 shows the gas desorption spectrum and the TG profile of a $BN^{nano}CH_x$–LiH composite (Li–BN–C–H composite), where the composite was synthesized from $BN^{nano}CH_x$ and LiH by ball-milling for 2 h and $BN^{nano}CH_x$ was chosen as being milled for 80 h. As shown in the TDMS spectrum of the Li–BN–C–H composite, the hydrogen desorption spectrum revealed some peaks corresponding to 200, 350 and above 500 °C. The hydrogen desorption intensity at each peak in the figure indicates that the amount of hydrogen desorption at 200 °C is much larger than

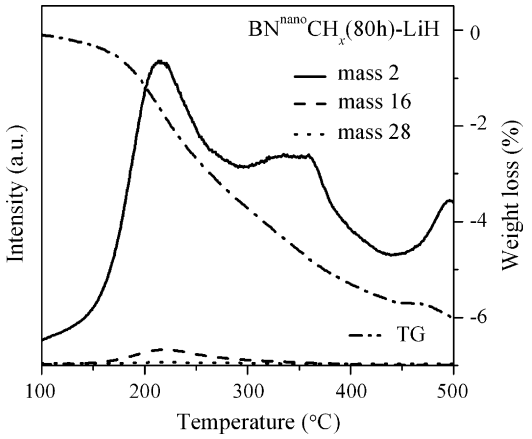


Fig. 4. Thermal gas desorption spectra of hydrogen (mass 2) and a small amount of hydrocarbons (mass 16 and 28) from the 80 h milled $BN^{nano}CH_x$–LiH composite and TG profile corresponding to weight loss (dashed and dotted line) with gases desorption.

those of other hydrogen desorption. It is noteworthy that this desorbing temperature at 200 °C is much lower than the decomposition temperatures of $BN^{nano}CH_x$ and LiH, which are above 400 and 650 °C, respectively. In addition, this hydrogen desorption from the $BN^{nano}CH_x$–LiH composite at 200 °C proceeds at much lower temperature than that from the $C^{nano}H_x$–LiH composite at 350 °C [10].

It is noticed that a small amount of hydrocarbons was desorbed around 200 °C as well, in which hydrocarbons desorption temperature was much lower than that of the $BN^{nano}CH_x$ itself. Furthermore, the amount of hydrocarbons emission from the $BN^{nano}CH_x$–LiH composite was obviously suppressed compared with hydrocarbons desorption from the $BN^{nano}CH_x$ material itself. Those results indicate that hydrogen atoms absorbed as hydrocarbon groups are released instead of hydrocarbons at 200 °C by interacting with LiH, where hydrocarbons should be desorbed above 400 °C from $BN^{nano}CH_x$. As shown in Fig. 4, the weight loss of the $BN^{nano}CH_x$–LiH composite is about 6.0 mass%, where this value includes a contribution from a small amount of hydrocarbon emissions. These results indicate that hydrogen is released from both the components by chemical interaction between $BN^{nano}CH_x$ and LiH. In the DTA measurement of this composite, any endo/exothermic reactions could not be observed in the measuring temperature range, indicating that the enthalpy changes ($\Delta H$) of those reactions for the nano-composite of $BN^{nano}CH_x$ and LiH are expected to be quite small.

As shown in upper profile of Fig. 5, it is found that some peaks corresponding to LiH are confirmed in the XRD profiles of the as-milled $BN^{nano}CH_x$–LiH composite. On the other hand, these peaks are strongly suppressed in the XRD profile of this composite after heating up to 500 °C as shown in lower angle in the Fig. 5. It is seemed that small peaks around 32° correspond to boron oxide ($B_2O_3$) as quite small amount of impurity. These results indicate that nano-structural composite $(LiBNC)^{nano}$ might be formed after hydrogen desorption with increasing temperature up to 500 °C, which is similar structural properties to that of the Li–C–H material [10].

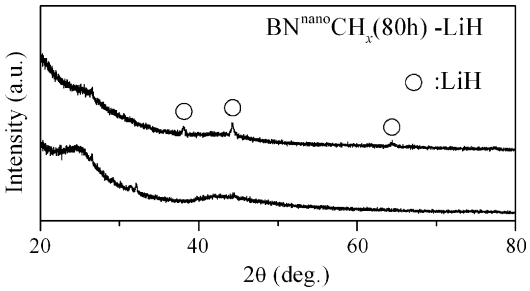


Fig. 5. The XRD profiles of the composite of the 80 h milled $BN^{nano}CH_x$–LiH after synthesizing by milling (upper) and after heating up to 500 °C (lower).

From above thermodynamic and structural properties of the $BN^{nano}CH_x$–LiH composite, it is considered that hydrogen in the both components are desorbed at lower temperature compared with the hydrogen desorption temperatures of $BN^{nano}CH_x$ and LiH by interaction between the polarized groups in the $BN^{nano}CH_x$ material and LiH in the nano-scale.

## 4. Conclusion

We have synthesized $BN^{nano}CH_x$ material and $BN^{nano}CH_x$–LiH nano-composite (Li–BN–C–H composite) by ball-milling method. The $BN^{nano}CH_x$ material possessed the polarized N–H, C–H and B–H groups at the edges of hexatomic ring structure in the nano-structural hBN layers synthesized during milling process under methane atmosphere. The hydrogen desorption temperatures of Li–BN–C–H composite were much lower than the hydrogen desorption temperatures of $BN^{nano}CH_x$ and LiH themselves. Moreover, the hydrocarbons emission from this composite at 200 °C was significantly suppressed compared with that of the $BN^{nano}CH_x$ material. Furthermore, the nano-structural cluster $(LiBNC)^{nano}$ was generated after hydrogen desorption with increasing up to 500 °C.

Thermodynamic and structural properties of Li–BN–C–H composite indicated that characteristic interaction existed between the polarized group in the $BN^{nano}CH_x$ material and ionic crystal of LiH in the nano-scale. This interaction led to a destabilization of hydrogenated states in $BN^{nano}CH_x$ and LiH.

## Acknowledgements

This work was supported by the Grant-in-Aid for COE Research of the Ministry of Education, Sciences and Culture of Japan and by the project “Development for Safe Utilization and Infrastructure of Hydrogen Industrial Technology” in NEDO, Japan.

## References

[1] A.C. Dillon, K.M. Jones, T.A. Bekkedahl, C.H. Kiang, D.S. Bethune, M.J. Heben, Nature 386 (1997) 377.
[2] S. Orimo, G. Majer, T. Fukunaga, A. Zuttel, L. Schlapbach, H. Fujii, Appl. Phys. Lett. 75 (1999) 3093.
[3] S. Orimo, T. Matsushima, H. Fujii, T. Fukunaga, G. Majer, J. Appl. Phys. 90 (2001) 1545.

[4] D.M. Chen, T. Ichikawa, H. Fujii, N. Ogita, M. Udagawa, Y. Kitano, E. Tanabe, J. Alloys Compd. 354 (2003) L5.
[5] S. Isobe, T. Ichikawa, J.I. Gottwald, E. Gomibuchi, H. Fujii, J. Phys. Chem. Solids 65 (2004) 535.
[6] T. Ichikawa, D.M. Chen, S. Isobe, E. Gomibuchi, H. Fujii, Mater. Sci. Eng. B: Solid State Mater. Adv. Technol. 108 (2004) 138.
[7] M. Hirscher, B. Panella, J. Alloys Compd. 404 (2005) 399.
[8] T. Fukunaga, K. Itoh, S. Orimo, K. Aoki, Mater. Sci. Eng. B: Solid State Mater. Adv. Technol. 108 (2004) 105.
[9] N. Ogita, K. Yamamoto, C. Hayashi, T. Matsushima, S. Orimo, T. Ichikawa, H. Fujii, M. Udagawa, J. Phys. Soc. Jpn. 73 (2004) 553.
[10] T. Ichikawa, H. Fujii, S. Isobe, K. Nabeta, Appl. Phys. Lett. 86 (2005).
[11] T. Ichikawa, S. Isobe, H. Fujii, Mater. Trans. 46 (2005) 1757.
[12] H. Miyaoka, T. Ichikawa, S. Isobe, H. Fujii, Phys. B: Conden. Matter 383 (2006) 51.
[13] H. Miyaoka, T. Ichikawa, H. Fujii, J. Alloys Compd. 432 (2007) 303.
[14] T. Ichikawa, N. Hanada, S. Isobe, H.Y. Leng, H. Fujii, J. Phys. Chem. B 108 (2004) 7887.
[15] C. Tang, Y. Bando, X. Ding, S. Qi, D. Golberg, J. Am. Chem. Soc. 124 (2002) 14550.
[16] R. Ma, D. Golberg, Y. Bando, T. Sasaki, Phil. Trans.: Math. Phys. Eng. Sci. (Ser. A) 362 (2004) 2161.
[17] X. Wu, J. Yang, J.G. Hou, Q. Zhu, J. Chem. Phys. 121 (2004) 8481.
[18] P. Wang, S. Orimo, T. Matsushima, H. Fujii, G. Majer, Appl. Phys. Lett. 80 (2002) 318.
[19] P. Wang, S. Orimo, H. Fujii, Appl. Phys. A: Mater. Sci. Process. 78 (2004) 1235.
[20] Y. Kojima, Y. Kawai, N. Ohba, J. Power Sources 159 (2006) 81.
[21] Y. Kojima, Y. Kawai, J. Alloys Compd. 395 (2005) 236.
[22] S. Isobe, T. Ichikawa, S. Hino, H. Fujii, J. Phys. Chem. B 109 (2005) 14855.
[23] P. Wang, S. Orimo, K. Tanabe, H. Fujii, J. Alloys Compd. 350 (2003) 218.